Journal of Earth Science, *Vol. 22*, *No. 5*, *p. 619–631*, *October 2011* *ISSN 1674-487X*
Printed in China
DOI: 10.1007/s12583-011-0213-6

Metasomatic Stages and Scapolitization Effects on Chemical Composition of Pasveh Pluton, NW Iran

S A Mazhari*
Department of Geology, *Payame Noor University*, *P.O. Box* 19395-4697, *Tehran*, *Iran*
S Amini
Department of Geology, *Tarbiat Moallem University*, 49 *Mofatteh Avenue*, *Tehran* 15614, *Iran*
J Ghalamghash
Geological Survey of Iran, *P.O. Box* 13195-1494, *Tehran*, *Iran*
F Bea
Department of Mineralogy and Petrology, *Fuentenueva Campus*, *University of Granada*, 18002 *Granada*, *Spain*

ABSTRACT: Pasveh gabbros are mafic component of a plutonic complex in the northwest Sanandaj-Sirjan Zone. These cumulative rocks are composed of plagioclase and calcic clinopyroxene (Cpx), which yield unusually high CaO (>19 wt.%) in whole-rock chemistry. Petrographical and geochemical data suggest that Pasveh gabbros can be divided into two groups: free scapolite and scapolite-bearing gabbros. The second group has higher Na_2O, K_2O, and P_2O_5 relative to free scapolite ones and is enriched in LIL (large ion lithophile) and HFS (high field strength) elements. Two stages of metasomatism affected the primary composition of mafic rocks. Firstly, high temperature reaction caused to invert primary high Ti clinopyroxene to low Ti clinopyroxene+high Ti amphibole. This reaction was extensive and included all gabbroic samples. Hydrothermal fluids involved in this process can be derived from dehydration reactions of country rocks or from other magmas incorporated in the formation of Pasveh complex pluton. The second metasomatic stage relates to scapolitization of limited parts of gabbroic rocks. An external saline fluid, which is composed of major NaCl and minor KCl and P_2O_5 components, impacted locally on Pasveh gabbros and formed the second metasomatic stage. Possible sources of Na and Cl are primary evaporites or brines, which were present in the host sediments of the gabbros. The carbonate-free nature of these hydrothermal fluids suggests that hydrothermal fluids responsible for the formation of scapolite in Pasveh gabbros are derived from marine evaporitic parentage.

KEY WORDS: Iran, Sanandaj-Sirjan Zone, Pasveh pluton, gabbro, metasomatism, high Ti Cpx, low Ti Cpx, amphibole, scapolite.

INTRODUCTION

Northwest (NW) Sanandaj-Sirjan Zone (SSZ), as an imbricated geological unit, consists of abundant plutonic assemblages. Since the most components of these plutons are granitoid, the major part of researches on these intrusives is restricted to felsic plutons. Nevertheless, mafic magmas appear throughout this zone and may play an important role in the petro-

*Corresponding author: ali54894@yahoo.com

Manuscript received December 13, 2009.
Manuscript accepted March 10, 2010.

genesis evolution of SSZ. Pasveh gabbros are one of the mafic intrusive bodies that outcrop on the limited area of Pasveh plutonic complex. This complex intruded ~40 Ma and the major plutonic rocks are calc-alkaline granitoids (Mazhari, 2008), which are similar to other granitoids in NW SSZ; in contrast to other mafic magmatic rocks that are calc-alkaline diorite or diorite-gabbros (e.g., Ghalamghash et al., 2009; Ahmadi-Khalaji et al., 2007), Pasveh gabbros are cumulative, which have mineralogical and geochemical signatures different from other mafic plutonic rocks in SSZ.

This article presents the first petrographical and geochemical study on Pasveh gabbros. These data show two different petrological groups. The probable conditions involved in the formation of this division are discussed in the next sections to access the best interpretation about various geochemical trends.

GEOLOGICAL SETTING

Pasveh pluton is located on NW SSZ, NW of Iran (Fig. 1). SSZ is a constituent of the Zagros orogen. The Zagros orogen, which resulted from the opening and closure of neo-Tethys Ocean, is composed of three NW elongated parallel tectonic zones (Alavi, 1994), which from the Arabian plate to Central Iran are (1) the Zagros simply folded belt to the SW, (2) the SSZ in the middle, and (3) the Urumieh-Dokhtar magmatic arc to the NE. The SSZ (recently renamed as the Zagros Imbricate Zone (Alavi, 2004)) contains numerous granite plutons, the age, nature, and origin of which are still poorly known. It is generally assumed that they are arc-related calc-alkaline granitoids formed during the subduction of neo-Tethys underneath the Iranian plate (e.g., Ghalamghash et al., 2009; Ahmadi-Khalaji et al., 2007). Our studies on the northern part of the SSZ, however, have revealed a more complicated picture. First, the radiometric age of intrusive bodies spans from ca. 300 Ma, prior to the beginning of the subduction, to 40 Ma, post-subduction (Mazhari et al., 2009; Mazhari, 2008). Second, in addition to the mentioned calc-alkaline plutons, there are other plutons mostly composed of alkaline rocks that hardly can be directly related to subduction (e.g., Piranshahr alkaline pluton (Mazhari et al., 2009)).

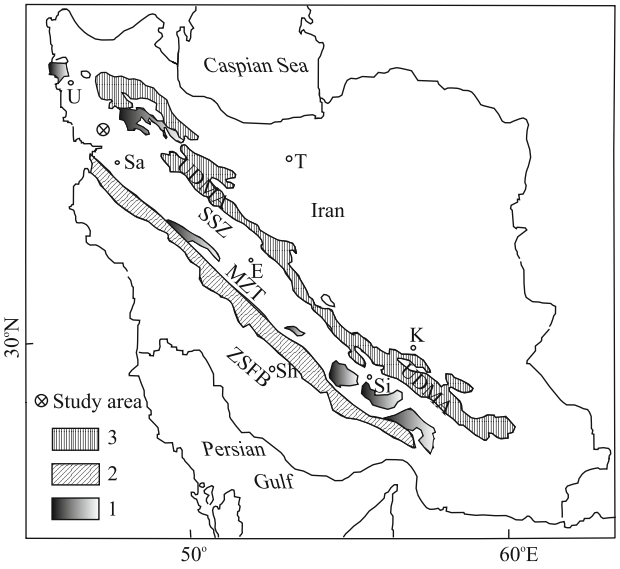

Figure 1. Zagros subdivision (after Alavi, 1994). 1. Precambrian basement; 2. Zagros thrust zone; 3. Urumieh-Dokhtar magmatic assemblage (arc) (UDMA). D. Dokhtar; E. Esfahan; K. Kerrman; MZT. Main Zagros thrust; Sa. Sanandaj; Si. Sirjan; Sh. Shihraz; SSZ. Sanandaj-Sirjan zone; T. Tehran; U. Urumieh; ZSFB. Zagros simply folded belt. Pasveh pluton is located as study area.

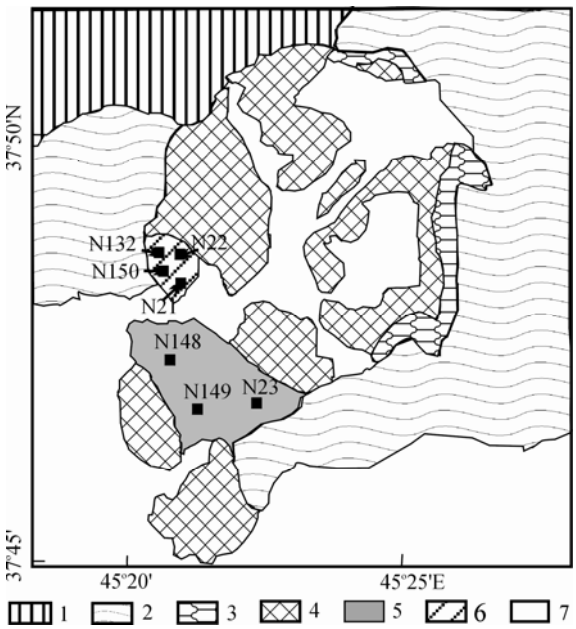

Figure 2. Geological map of Pasveh plutonic complex. 1. Permian carbonates; 2. Cretaceous sedimentary rocks; 3. contact metamorphic rocks; 4. granitoids; 5. free scapolite gabbros; 6. scapolite-bearing gabbros+free scapolite gabbros; 7. Quaternary alluvium. The locations of analyzed samples are shown.

Pasveh pluton is a plutonic complex that is composed of two distinct felsic and mafic rocks and located between 45º20′E–45º27′E and 37º45′N–37º52′N. This complex intruded to Permian and Mesozoic sedimentary rocks (Eftekharnejad, 1973; Fig. 2). Mafic and felsic rocks are not cogenetic and have diverse petrogenetic history. Felsic rocks occupy major parts of pluton and consist of various calc-alkaline granitoid rocks with different compositions. They differ from granite to granodiorite, quartz diorite, and tonalite, which include a lot of enclave especially mafic microgranular enclave (MME) in more mafic rocks. U-Pb SHRIMP analyses on zircon grains show discordia intercept age of 39.83±1.07 Ma, and isotopic data show that magma mixing and fractional crystallization processes had an important role in the production of various granitoids (Mazhari, 2008). Mafic magma appears as gabbroic rocks in the middle parts of the Pasveh complex. They have been divided to two sections on the basis of presence or absence of scapolite in Fig. 2. In the southern unit, there is only free scapolite gabbro, but in the northern unit there are limit areas that contain scapolite-bearing gabbros. U-Pb SHRIMP data suggested 40.63±0.84 Ma for the generation age (Mazhari, 2008). These rocks have unusual characteristics relative to other mafic magmas in calc-alkaline plutons of SSZ (see below).

SAMPLES AND METHODS

We collected 7 samples representative of whole Pasveh gabbros. These include 4 free scapolite gabbros (N22, N23, N148, and N149) and 3 scapolite-bearing rocks (N21, N132, and N150). All samples were analyzed for major and 39 trace elements, including 14 REEs, Th, and U. Thin sections of the whole collection were studied under the optical microscope. Two samples (N21 and N23) were also studied with the scanning electron microscope with backscattered electrons (to identify accessories) and electron microprobe for mineral analysis.

Whole-rock major-element and Zr determinations were done by X-ray fluorescence after fusion with lithium tetraborate. Typical precision was better than ±1.5% for an analyte concentration of 10 wt.% and ±2.5% for 100 ppm Zr. Trace elements were determined by ICP-mass spectrometry (ICPMS) after HNO_3+HF digestion of 0.100 0 g sample powder in a Teflon-lined vessel at ~180 ℃ and ~200 psi for 30 min, evaporation to dryness, and subsequent dissolution in 100 mL of 4 vol.% HNO_3; the precision was better than ±5% for analyte concentrations of 10 ppm. The concentration of Hf was calculated from the ICP-MS Zr/Hf and the XRF Zr concentration.

Major-element analyses of minerals were obtained by wavelength dispersive analyses with a CAMECA SX100 electron microprobe using the natural and synthetic standards. Accelerating voltage was 20 kV and beam current was 20 nA. The precision was close to ±4% for an analyte concentration of 1 wt.%. All of these analyses were done in Granada University, Spain.

PETROGRAPHY

The Pasveh gabbro is medium grain size (1–3 mm) and dark grey massive rock, which has restricted outcrop in this plutonic complex (Fig. 2). Texturally, gabbros are cumulative rocks of plagioclase and clinopyroxene (Cpx). Plagioclase appears as euhedral to anhedral crystals and forms 20% to 40% of these rocks. Clinopyroxene is the major constituent of gabbros (50%–70%), which fills plagioclase interstice or occurs as anhedral poikiloblasts enclosing plagioclases (Figs. 3a and 3b). Observed textures in gabbroic samples suggest that cumulus plagioclases crystallized firstly, and then Cpx formed inter cumulus textures. Interaction relations between plagioclase and Cpx show that plagioclase continues to crystallize after it. Primary minor minerals include apatite, Fe-Ti oxides, titanite, and rare small grains of zircon.

Detail consideration of textural relations indicated that subsolidus processes play an important role in mineralogical composition of these rocks. With this regard, it is possible to divide gabbroic samples into two subgroups: free scapolite gabbros (samples of N22, N23, N148, and N149) and scapolite-bearing gabbros (N21, N132, and N150). Detailed mineralogical properties of these rocks are discussed below.

Free Scapolite Gabbros

The major volume of mafic rocks consists of this group. Primary components contain cumulus plagioclase crystals, which are enclosed by interstitial Cpx.

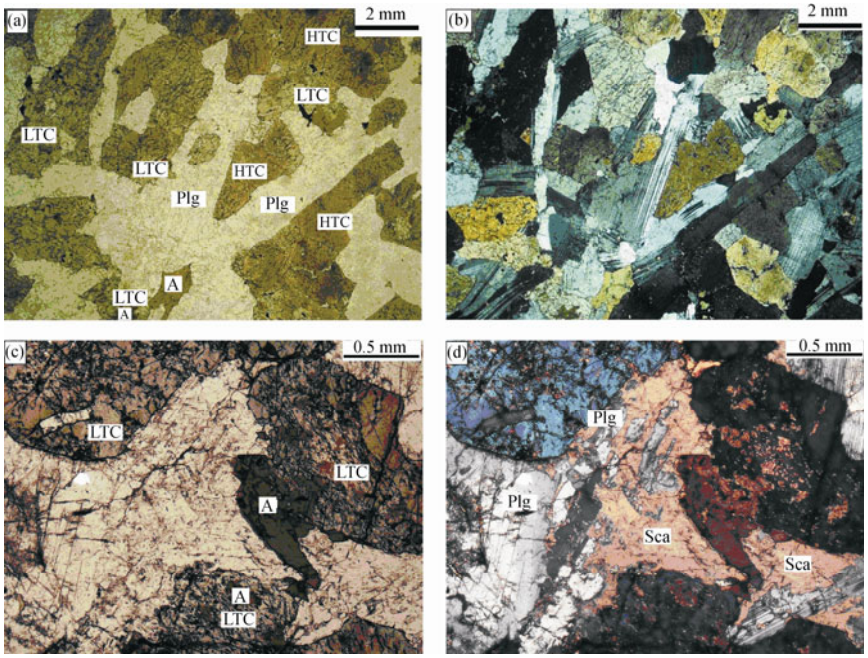

Figure 3. (a) Free scapolite gabbro with euhedral to subhedral plagioclases enclosed by clinopyroxene. Conversion of high Ti clinopyroxene (HTC) to low Ti clinopyroxene (LTC) and brown amphibole (A) are distinguished. (b) Picture (a) in XPL. (c) Scapolite-bearing gabbro in PPL. (d) The same picture in XPL. Plagioclase (Plg) replaced partially by scapolite (Sca). There are relicts of plagioclase fragments in scapolite.

Table 1 Representative analyses of plagioclase in Pasveh gabbros (wt.%)

Sample ID	N23	N23	N23	N23	N23	N21	N21	N21
Type of rock	FG	FG	FG	FG	FG	SG	SG	SG
SiO_2	50.64	50.03	47.77	46.58	45.22	50.72	54.70	54.02
TiO_2	0.03	0.04	0.10	0.01	0.00	0.05	0.05	0.06
Al_2O_3	31.31	31.67	33.34	34.38	35.06	31.55	29.24	29.56
FeO	0.18	0.22	0.39	0.10	0.19	0.37	0.28	0.26
CaO	14.18	14.72	16.53	17.61	18.52	13.99	11.00	11.64
Na_2O	3.52	3.23	2.17	1.56	1.03	3.34	4.98	4.65
K_2O	0.09	0.08	0.05	0.02	0.02	0.15	0.28	0.28
Total	99.95	99.99	100.35	100.26	100.04	100.17	100.53	100.47
Structural formula (8O)								
Si	2.31	2.28	2.19	2.14	2.09	2.31	2.46	2.43
Ti	0.00	0.00	0.00	0.00	0.00	0.00	0.00	0.00
Al	1.68	1.70	1.80	1.86	1.91	1.69	1.55	1.57
Fet	0.01	0.01	0.01	0.00	0.01	0.01	0.01	0.01
Ca	0.69	0.72	0.81	0.87	0.92	0.68	0.53	0.56
Na	0.31	0.29	0.19	0.14	0.09	0.29	0.43	0.41
K	0.01	0.00	0.00	0.00	0.00	0.01	0.02	0.02
Ab	30.84	28.29	19.14	13.80	9.13	29.90	44.29	41.27
An	68.64	71.25	80.57	86.08	90.75	69.21	54.07	57.09
Or	0.52	0.46	0.29	0.12	0.12	0.88	1.64	1.64

FG. free scapolite; SG. scapolite-bearing samples.

Table 2 Selected EPM analyses of clinopyroxenes in Pasveh mafic rocks (wt.%)

Sample ID	N21	N21	N21	N21	N23	N23	N23	N23
Type of rock	SG	SG	SG	SG	FG	FG	FG	FG
SiO_2	52.31	50.51	49.17	48.13	51.83	50.60	46.99	45.64
TiO_2	0.16	0.54	1.38	1.84	0.33	0.75	2.69	3.09
Al_2O_3	1.09	2.86	4.08	4.74	1.62	3.06	6.24	7.24
Cr_2O_3	0.00	0.02	0.19	0.03	0.00	0.03	0.01	0.00
NiO	0.00	0.01	0.03	0.00	0.00	0.02	0.00	0.01
FeO	10.66	11.66	11.39	11.09	10.93	8.37	9.33	10.48
MnO	0.26	0.26	0.26	0.22	0.15	0.16	0.14	0.15
MgO	11.78	10.82	10.63	10.62	11.55	12.55	10.93	10.41
CaO	23.70	22.97	22.33	22.65	23.91	24.07	23.35	23.03
Na_2O	0.28	0.52	0.68	0.58	0.34	0.42	0.61	0.61
K_2O	0.02	0.02	0.02	0.01	0.02	0.04	0.02	0.00
F	0.09	0.08	0.13	0.17	0.16	0.10	0.15	0.08
Cl	0.01	0.02	0.00	0.00	0.01	0.08	0.01	0.01
Total	100.37	100.31	100.30	100.09	100.86	100.24	100.48	100.76
Structural formula (6O)								
Si	1.97	1.91	1.85	1.82	1.94	1.89	1.76	1.71
Ti	0.00	0.02	0.04	0.05	0.01	0.02	0.08	0.09
Al	0.05	0.13	0.18	0.21	0.07	0.13	0.28	0.32
Cr	0.00	0.00	0.01	0.00	0.00	0.00	0.00	0.00
Ni	0.00	0.00	0.00	0.00	0.00	0.00	0.00	0.00
Fet	0.34	0.37	0.36	0.35	0.34	0.26	0.29	0.33
Mn	0.01	0.01	0.01	0.01	0.00	0.01	0.00	0.00
Mg	0.66	0.61	0.60	0.60	0.65	0.70	0.61	0.58
Ca	0.95	0.93	0.90	0.92	0.96	0.96	0.94	0.92
Na	0.02	0.04	0.05	0.04	0.02	0.03	0.04	0.04
K	0.00	0.00	0.00	0.00	0.00	0.00	0.00	0.00
F	0.01	0.01	0.02	0.02	0.02	0.01	0.02	0.01
Cl	0.00	0.00	0.00	0.00	0.00	0.01	0.00	0.00
Fe^{3+}	0.04	0.08	0.09	0.11	0.07	0.10	0.12	0.14
Fe^{2+}	0.29	0.29	0.27	0.24	0.27	0.16	0.18	0.19
En	0.34	0.32	0.32	0.32	0.33	0.36	0.33	0.32
Wo	0.49	0.49	0.49	0.49	0.49	0.50	0.51	0.50
Fs	0.17	0.19	0.19	0.19	0.18	0.14	0.16	0.18

FG. free scapolite; SG. scapolite-bearing samples.

Plagioclase contains both homogenous and zoned crystals and its composition ranges from An_{69} to An_{91} (Table 1). Clinopyroxenes originally have pink colour with high CaO (23 wt.%–24 wt.%), TiO_2 (1.38 wt.%–3.10 wt.%), and Al_2O_3 (4.49 wt.%–7.32 wt.%) (Figs. 3a and 3b and Table 2). On the basis of pyroxene nomenclature (Morimoto, 1989), all clinopyroxenes have diopside composition.

An extensive reaction that affects all samples has formed secondary pyroxenes and amphiboles. Petrographical evidence shows high Ti Cpx (HTC) replaced by low Ti Cpx (LTC)+relatively high Ti amphibole+ titanite+Fe-Ti oxides. The extent of this reaction is not uniform, so that in some cases reaction appears in

small part of primary Cpx but in other issues all clinopyroxenes replaced by new minerals (Fig. 3). New clinopyroxenes are diopside in composition, too, but show distinct features from primary minerals (Fig. 4). They are colourless and contain low TiO_2 (0.33 wt.%–0.75 wt.%) and Al_2O_3 (1.62 wt.%–3.06 wt.%) (Table 2 and Fig. 3). Amphiboles are brown with relatively high TiO_2 (2.81 wt.%–4.12 wt.%) and variable Cl (0.08 wt.%–0.96 wt.% with mean 0.53 wt.%) (Table 3). They have hastingsite-pargasite composition in the amphibole classification (Leake et al., 1997).

Table 3 Representative analyses of amphiboles in Pasveh gabbros (wt.%)

Sample ID	N21	N21	N21	N21	N23	N23	N23	N23
Type of rock	SG	SG	SG	SG	FG	FG	FG	FG
SiO_2	38.14	38.05	38.01	38.58	39.24	38.77	38.48	40.07
TiO_2	2.83	2.84	2.98	2.77	3.45	3.24	3.47	3.43
Al_2O_3	13.01	12.93	13.03	12.74	13.02	13.09	12.84	12.39
Cr_2O_3	0.02	0.00	0.01	0.05	0.03	0.03	0.00	0.00
NiO	0.00	0.00	0.00	0.02	0.00	0.04	0.00	0.01
FeO	20.80	21.53	21.19	20.50	19.02	19.10	19.92	15.80
MnO	0.22	0.31	0.29	0.24	0.16	0.12	0.12	0.15
MgO	7.04	6.75	7.22	7.13	7.96	8.25	7.33	10.40
CaO	11.33	11.49	11.46	11.53	11.90	11.84	11.94	12.09
Na_2O	1.78	1.62	1.85	1.70	2.88	2.44	2.11	2.43
K_2O	2.40	2.50	2.39	2.54	0.76	1.32	1.85	1.42
F	0.30	0.21	0.27	0.26	0.35	0.29	0.27	0.33
Cl	0.80	0.73	0.43	0.87	0.13	0.75	0.73	0.16
Total	98.67	98.97	99.13	98.92	98.89	99.28	99.05	98.68
Structural formula (23O)								
Metodos	13NCK	13NCK	13NCK	13NCK	13NCK	13NCK	13NCK	13NCK
Factor	9.33	9.33	9.26	9.33	9.18	9.18	9.31	9.07
Si	5.92	5.91	5.86	5.99	5.99	5.93	5.96	6.05
Ti	0.33	0.33	0.35	0.32	0.40	0.37	0.40	0.39
Al	2.38	2.37	2.37	2.33	2.34	2.36	2.34	2.20
Cr	0.00	0.00	0.00	0.01	0.00	0.00	0.00	0.00
Ni	0.00	0.00	0.00	0.00	0.00	0.00	0.00	0.00
Fe^{3+}	0.68	0.65	0.66	0.54	0.18	0.52	0.28	0.22
Fe^{2+}	2.02	2.14	2.07	2.13	2.25	1.92	2.30	1.78
Mn	0.03	0.04	0.04	0.03	0.02	0.02	0.02	0.02
Mg	1.63	1.56	1.66	1.65	1.81	1.88	1.69	2.34
Ca	1.89	1.91	1.89	1.92	1.95	1.94	1.98	1.96
Na	0.54	0.49	0.55	0.51	0.85	0.72	0.63	0.71
K	0.48	0.49	0.47	0.50	0.15	0.26	0.37	0.27
F	0.15	0.10	0.13	0.13	0.17	0.14	0.13	0.16
Cl	0.21	0.19	0.11	0.23	0.03	0.19	0.19	0.04
T Otten	943.00	944.00	960.00	934.00	985.00	979.00	987.00	983.00

FG. free scapolite; SG. scapolite-bearing samples. T Otten is calculated temperature on the basis of Ti in amphibole (see text).

Scapolite-Bearing Gabbros

Scapolitization on Pasveh gabbros manifests only in the limited location on the northern part of mafic rocks (Fig. 2). These rocks are mineralogically and texturally similar to free-scapolite type, except of the occurrence of scapolite and increase of secondary titanite and opaque minerals. Primary pyroxene in this kind of gabbro has lower TiO_2 (1.09 wt.%–1.89 wt.%). Scapolite is formed in the expense of plagioclase (Figs. 3c and 3d). The extension of scapolitization is not complete and in the highest contents, 20% of feldspars altered to scapolite (the samples of N21 and N150) and in the sample of N132 only 5% of feldspars are replaced by scapolite. Often, the scapolite is seen spreading through the feldspar, portions being completely replaced, while others are still fresh and unaltered. As scapolite crystals invade plagioclase laths, they are partially but not totally restricted to paths along cleavage planes and are not restricted to particular plagioclase compositional zones. The feldspar is not weathered and remains fresh and are more sodic (An_{54}–An_{69}) than free scapolite rocks (Table 1). Scapolite composition and its production conditions (Table 4) will be explained later.

Table 4 Selected EPM analyses of scapolites in Pasveh mafic rocks (wt.%)

Sample ID	N21	N21	N21	N21	N21	N21	N21
SiO_2	52.85	53.09	52.74	53.18	52.86	52.72	53.23
TiO_2	0.01	0.03	0.01	0.00	0.00	0.00	0.01
Al_2O_3	24.84	24.67	24.49	24.51	24.56	24.78	24.54
Cr_2O_3	0.02	0.00	0.03	0.01	0.00	0.03	0.05
FeO	0.11	0.10	0.14	0.19	0.19	0.13	0.07
MnO	0.00	0.03	0.03	0.00	0.00	0.00	0.00
MgO	0.00	0.00	0.01	0.00	0.00	0.01	0.00
CaO	9.42	9.31	9.47	9.25	9.23	9.61	8.82
Na_2O	7.72	7.71	7.78	7.90	7.83	7.52	8.10
K_2O	1.28	1.38	1.35	1.44	1.28	1.40	1.15
F	0.06	0.00	0.03	0.08	0.03	0.05	0.07
Cl	4.83	4.99	4.85	4.91	4.96	4.81	4.94
Total	101.14	101.31	100.93	101.47	100.94	101.06	100.98
Structural formula (24O)							
Si	7.72	7.75	7.76	7.78	7.75	7.72	7.78
Ti	0.00	0.00	0.00	0.00	0.00	0.00	0.00
Al	4.28	4.25	4.24	4.22	4.25	4.28	4.22
Cr	0.00	0.00	0.00	0.00	0.00	0.00	0.01
Fe	0.01	0.01	0.02	0.02	0.02	0.02	0.01
Mn	0.00	0.00	0.00	0.00	0.00	0.00	0.00
Mg	0.00	0.00	0.00	0.00	0.00	0.00	0.00
Ca	1.48	1.46	1.49	1.45	1.45	1.51	1.39
Na	2.19	2.19	2.22	2.24	2.23	2.14	2.30
K	0.24	0.26	0.25	0.27	0.24	0.26	0.22
F	0.03	0.00	0.01	0.04	0.01	0.02	0.03
Cl	1.20	1.24	1.21	1.22	1.24	1.19	1.23
X_{Me}	37.81	37.38	37.64	36.62	37.03	38.62	35.50
X_{EqAn}	42.85	41.78	41.33	40.85	41.76	42.69	41.32
EPC	1.13	1.14	1.26	1.23	1.17	1.17	1.07

Table 5 Whole-rock analyses of gabbroic rocks of Pasveh pluton

Sample ID	N23	N148	N149	N22	N132	N150	N21
Type of rock	FG	FG	FG	FG	SG	SG	SG
SiO_2	46.01	46.42	48.23	48.35	47.67	49.14	49.89
TiO_2	1.44	1.44	1.02	1.05	1.24	1.13	1.14
Al_2O_3	17.62	17.65	16.70	16.42	17.08	16.58	16.57
FeOt	6.53	6.50	5.04	5.23	6.09	6.26	6.24
MgO	5.92	5.80	7.02	7.26	5.84	4.51	4.50
MnO	0.08	0.09	0.09	0.09	0.10	0.12	0.12
CaO	19.40	19.23	18.81	19.08	18.45	16.60	16.44
Na_2O	0.80	0.96	1.15	1.22	1.42	2.42	2.42
K_2O	0.07	0.13	0.09	0.13	0.27	0.69	0.71
P_2O_5	0.03	0.11	0.04	0.05	0.27	0.79	0.80
LOI	0.51	0.26	0.43	0.95	0.38	0.69	0.75
Li	6.53	6.59	3.43	4.15	6.73	10.11	10.58
Rb	1.66	2.70	1.94	1.73	5.54	11.87	11.88
Cs	0.44	0.26	0.19	0.35	0.19	0.51	0.59
Be	0.33	0.37	0.42	0.44	0.58	1.02	1.03
Sr	502.64	514.94	499.25	481.02	535.41	644.27	640.53
Ba	37.70	52.16	42.78	42.29	73.94	151.10	149.28
Sc	37.08	37.16	41.80	42.58	35.94	26.97	27.57
V	247.04	237.95	222.28	226.51	216.95	170.49	174.59
Cr	25.84	16.37	319.10	335.42	115.38	38.82	39.61
Co	29.97	29.00	25.89	25.29	24.99	20.72	20.47
Ni	31.67	40.50	62.56	79.67	32.24	30.91	20.39
Cu	8.34	7.40	41.28	43.92	18.69	15.48	16.83
Zn	35.92	39.26	29.83	33.31	44.37	62.24	67.57
Ga	16.60	16.91	14.10	14.56	16.33	17.36	17.38
Y	10.86	11.86	12.53	12.92	15.92	27.34	27.83
Nb	1.81	1.87	0.92	1.72	3.71	10.43	11.25
Ta	0.09	0.18	0.13	0.06	0.36	0.81	0.75
Zr	54.00	61.10	46.70	50.90	72.10	113.00	114.80
Hf	2.05	2.10	1.70	1.57	2.40	3.10	3.13
Mo	0.23	0.25	0.17	0.07	0.27	0.75	0.72
Sn	0.64	1.04	0.48	0.08	0.97	1.15	1.18
Tl	0.02	0.01	0.01	0.03	0.02	0.04	0.06
Pb	2.36	2.75	1.20	1.38	4.11	9.21	9.06
U	0.06	0.14	0.06	0.07	0.33	0.96	1.01
Th	0.14	0.39	0.19	0.37	1.06	2.82	2.97
La	2.73	3.95	3.01	3.21	7.60	18.38	19.21
Ce	6.54	9.61	8.37	8.18	17.14	39.76	41.22
Pr	1.07	1.51	1.37	1.29	2.42	5.22	5.32
Nd	5.33	7.09	7.04	6.50	11.07	21.97	23.08
Sm	1.78	2.06	2.11	2.00	2.91	5.37	5.35

Continued

Sample ID	N23	N148	N149	N22	N132	N150	N21
Type of rock	FG	FG	FG	FG	SG	SG	SG
Eu	0.78	0.84	0.91	0.95	1.03	1.70	1.86
Gd	2.21	2.20	2.46	2.65	3.19	5.29	5.64
Tb	0.33	0.37	0.41	0.41	0.51	0.84	0.88
Dy	1.93	2.34	2.48	2.51	3.12	5.05	5.45
Ho	0.39	0.46	0.47	0.49	0.59	1.01	1.05
Er	1.02	1.24	1.20	1.16	1.51	2.58	2.81
Tm	0.15	0.17	0.17	0.17	0.22	0.36	0.39
Yb	0.95	1.07	1.12	1.02	1.44	2.17	2.37
Lu	0.14	0.16	0.18	0.16	0.21	0.32	0.34

FG. free scapolite; SG. scapolite-bearing samples; LOI. losses of ignition. Unit is wt.% for major elements and ppm for minor elements.

CHEMICAL COMPOSITION

Whole-rock geochemical data of gabbroic rocks are presented in Table 5. With respect to major oxides, all rocks show relatively homogenous composition with limited variations. Very high content of CaO, especially in free scapolite group (>19 wt.%), attests to cumulative nature of these rocks due to high content of calcic Cpx and plagioclase. Al_2O_3 is high (16.42 wt.%–17.45 wt.%), too. Scapolite-bearing samples show enrichment in Na_2O, K_2O, and P_2O_5 relative to free scapolite gabbros.

Minor and trace elements exhibit completely different abundances so that LILE and HFSE show several times enrichment in scapolite-bearing samples. Therefore, rare earth elements diagram shows different trends in these two groups (Fig. 5). Free scapolite samples show flat REE pattern [$(La/Yb)_N$=1.82–2.48] with positive Eu anomaly (Eu/Eu*=1.20–1.26). REE abundance in free scapolite rocks is low (sum REE=25.34–33.07), while scapolite-bearing gabbros contain higher values (sum REE=52.95–114.96) and steeper trend [$(La/Yb)_N$=3.57–5.71] without Eu anomaly (Eu/Eu*=0.98–1.04). Primary mantle normalized spider diagram (Fig. 6) clears another differences between these two groups. Free scapolite gabbros show positive Ti and negative P anomaly in contrast to scapolite-bearing samples that demonstrate reverse situation. By comparison of these trends and raw data in Table 5, it is understood that positive P anomaly in scapolite-bearing rocks on spider diagrams

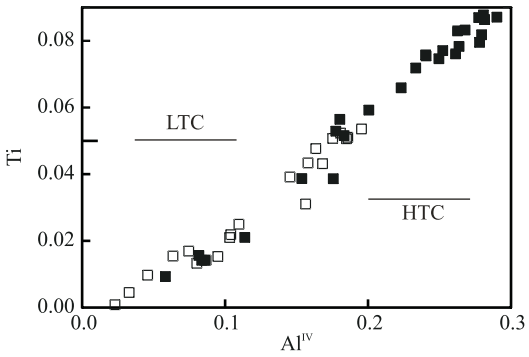

Figure 4. Variation of clinopyroxene compositions in terms of Ti and Al^{IV}. Clinopyroxenes with different petrographic characteristic (see text) show two distinguishable groups: low Ti clinopyroxene (LTC) and high Ti clinopyroxene (HTC). □. Scapolite-bearing samples; ■. free scapolite samples.

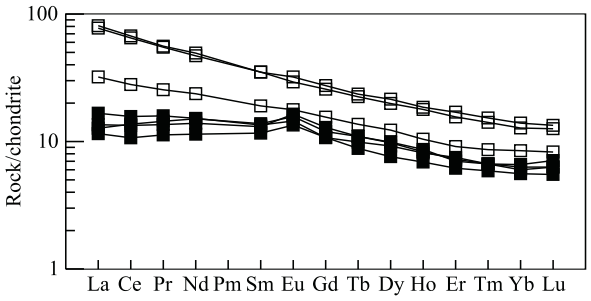

Figure 5. Chondrite normalized diagram of REE for gabbroic rocks in Pasveh complex. □. Scapolite-bearing samples; ■. free scapolite samples. Normalizing values are from Sun and McDonough (1989).

resulted due to enrichment of this element in these rocks, but negative Ti anomaly was caused by increase of adjacent elements (Eu and Dy), not Ti decrease.

DISCUSSION

Mafic rocks on Pasveh plutons are affected by two reaction stages. The first stage that is extensive and includes all samples yielded the transformation of high Ti Cpx to low Ti Cpx and high Ti amphibole, but the second is restricted to limited locations and related to scapolitization of plagioclases. Here, the conditions and probable factors that could be effective during these reactions will be discussed.

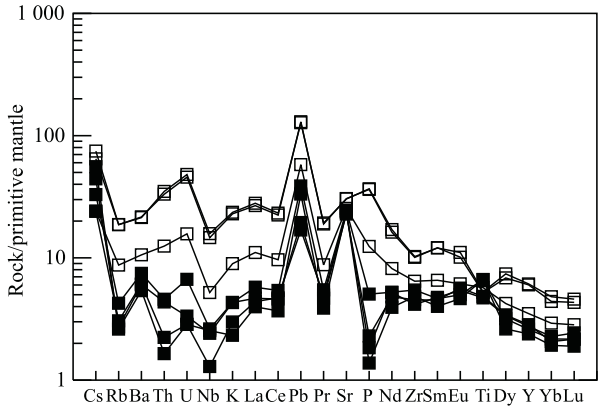

Figure 6. Primitive mantle-normalized multi-element plots for Pasveh gabbros. □. Scapolite-bearing samples; ■. free scapolite samples. Normalizing values are from Sun and McDonough (1989).

First Stage: Late Magmatic Stage or High Temperature Metasomatism?

The production of secondary LTC (low Ti Cpx) in gabbroic rocks has been reported by some authors. For example, Vanko and Bishop (1982) suggested that secondary low Ti, Al clinopyroxenes in Humboldt Lopolith, Nevada, formed by hydrothermal effects tend to alter the composition of primary clinopyroxenes (Vanko and Bishop, 1982). It seems that the generation of LTC in Pasveh gabbro was yielded by such process. Brown amphiboles similar to Pasveh pargasite and hastingsites are common minor minerals in such gabbroic rocks (e.g., Otten, 1984; Vanko and Bishop, 1982). There is no consensus about the genesis of these minerals. Vanko and Bishop (1982) describe them as a result of increased chlorine activity as early as the late magmatic stage because of their high chlorine content (>0.5 wt.%), while Otten (1984) believes that similar amphiboles in Artfjället gabbro, Sweden, are not magmatic and have subsolidus origin. To understand which conditions are true for Pasveh gabbros, it is necessary to consider textural relations carefully. The replacement of HTC by amphibole and LTC can be seen as different forms: usually replacement occurs as oikocrysts of LTC enclosing amphiboles (Fig. 3), this substitution can be partially or completely; in minor cases, LTC and amphibole occur independently so that LTC occupies some parts or whole HTC, and amphibole appears in the rims of HTC or as blebs in it (Fig. 3). These relations show that LTC and amphibole should be formed at the same conditions. Furthermore, textural occurrences are more similar to metasomatic positions than magmatic because usually amphiboles and LTC appear as metasomatic points and spots in HTC. Hence, it seems that the production of LTC and amphibole are due to subsolidus reactions. A relatively high Cl fluid may affect primary pyroxenes and convert them to secondary LTC and brown amphibole. The metasomatic nature of these minerals does not mean low temperature of their production. Some evidence shows high *T* for the formation of them as discussed below.

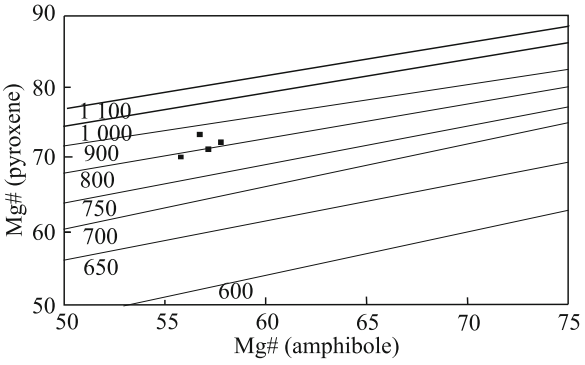

Figure 7. Amphibole-pyroxene graphical thermometry of Pasveh gabbros. Mg#=$Mg^{2+}/(Mg^{2+}+Fe^{2+})$.

Based on the partitioning of Mg/Fe, clinopyroxene-amphibole thermometer has been presented in graphical form with no information about the nature or quality of calibration (Perchuck et al., 1985).

Figure 7 shows application of this thermometry for Pasveh gabbros. Unfortunately, most of brown amphiboles have Mg#<50 and cannot plot on this diagram. Nevertheless, limited plotted data show >800 ℃, too. These results prove that metasomatic reaction of Pasveh gabbros responsible for the alteration of primary HTC to LTC+high Ti amphibole took place in high temperature. Hydrothermal fluids involved in this process can be derived from dehydration reactions of country rocks or from other magmas incorporated on the formation of Pasveh complex pluton. Although the latter probability is more reasonable, detailed study of fluid inclusion and stable isotopes is necessary to distinguish the major factor.

Second Stage: Scapolitization Metasomatism

The mineral scapolite is found in a wide variety of metamorphic and igneous rocks that have been altered by interactions with crustal fluids. Its general formula can be described by $(Na,Ca,K)_4(Al,Si)_6Si_6O_{24}(Cl,CO_3,SO_4)$. Two common end-members are called marialite ($Na_4ClSi_9Al_3O_{24}$) and meionite ($Ca_4CO_3Si_6Al_6O_{24}$). Scapolite is a potential indicator of the activities of volatile components (e.g., Cl, CO_2, and SO_3) during crustal processes because of its ability to incorporate these volatiles (e.g., Kullerud and Erambert, 1999; Jiang et al., 1994). For this reason, a lot of studies have been performed to define various aspects of scapolite (e.g., Seto et al., 2004; Teerstra and Sherriff, 1997; Komada et al., 1996; Baker and Newton, 1995; Chamberlain et al., 1985).

Scapolite plays as an important role in the second stage of metasomatism processes in Pasveh gabbros. EPMA analyses and cation calculation of scapolites are given in Table 4 on the basis of Teerstra and Sherriff (1997) method. Our analyses do not contain SO_2 and it is not possible to analyze CO_2 by EPMA. Nevertheless, by consideration of data on Table 4, it should be estimated that the content of SO_2 and CO_2 is insignificant: On the basis of Teerstra and Sherriff (1997), an excess positive charge (EPC) is calculated by subtracting the negative charge generated by the framework (TO_2^-) from the monovalent positive charge of the M cations (M^+) as follows: $EPC=M^+–TO_2^-$ where $M^+=Na+K+2(Ca+Mg+Sr+Ba+Mn+Fe^{2+})$ and $TO_2^-=Al+Fe^{3+}$. Since ΣM in the cation calculations is <4 apfu, Fe^{3+} has not been inserted on the Pasveh scapolites. This excess positive charge should be balanced by negative anions (S^{2-}, Cl^-, and CO_2). Calculation of EPC (Table 4) shows that all this positive charge can be balanced by Cl and the percentage of SO_2 and CO_2 must be negligible in Pasveh gabbro scapolites. Therefore, scapolites in Pasveh gabbros are without CO_2 components that have intermediate composition between marialite and meionite with X_{Me}=35.5–37.8 and X_{EqAn}=40.8–42.7 (X_{Me}=Ca/(Na+K+Ca) and X_{EqAn}=(Al − 3)/3 (e.g., Kullerud and Erambert, 1999; Komada et al., 1996)).

As mentioned in previous sections, plagioclase composition in scapolite-bearing gabbros is more sodic relative to plagioclase in free scapolite rocks; with respect to the composition of scapolite, it is resulted that a NaCl-bearing fluid reacted with plagioclase and produced scapolite. Moreover, increase of P_2O_5 and K_2O in whole rock (Table 5) and apatite abundance of scapolite-bearing rocks suggest that this fluid contains worthwhile amount of phosphor and potassium. Another function of these metasomatic stages is the formation of more titanite and Fe-Ti oxides in the expense of pyroxenes and amphiboles (HTC and brown amphibole in scapolite-bearing gabbros have lower Ti relative to other gabbros (Tables 2 and 3)). The evidence suggests that an external saline fluid impacted locally on Pasveh gabbros and yielded the second metasomatic stage. This fluid consisted of the major NaCl component and notable KCl and P_2O_5. Possible sources of Na and C1 fixed in secondary more sodic plagioclase and scapolite are primary evaporites or brines that were present in the sediments intruded by the gabbros. Carbonate-free nature of these hydrothermal fluids can be used to define the type of evaporitic sediments. Non-marine evaporitic sediments may give rise to carbonate-rich scapolites since non-marine parageneses often yield abundant sodium and calcium carbonates rather than halides and sulfates; therefore, hydrothermal fluids responsible for the formation of scapolite in Pasveh gabbros are derived from marine evaporitic parentage. There are occurrences of these evaporitic rocks in country rocks (Cretaceous sedimentary rocks; Fig. 2).

CONCLUSION

Mafic magma in Pasveh plutonic complex consists of cumulative gabbros composed of plagioclase and clinopyroxene. Two stages of metasomatism took place in gabbros. The first high temperature phase has transformed HTC to LTC+high Ti amphibole in addition to the formation of some titanite and Fe-Ti oxides. Hydrothermal fluids involved in this stage had enough Cl and derived from other contemporaneous magmas in Pasveh complex or derived by dehydration reaction with country rocks. This stage is extensive and includes all Pasveh gabbros.

The second stage contains scapolite formation in the limited location of Pasveh gabbros. High NaCl-bearing saline fluids derived from marine evaporitic sedimentary country rocks affected these rocks and altered their plagioclase to scapolite or more sodic plagioclases. Scapolite composition shows that CO_2 was absent during this stage. Other evolution of this stage is the increase of titanite and Fe-Ti oxides, decrease of Ti in HTC and amphiboles, and increase of K_2O and P_2O_5 in whole-rock composition of gabbroic rocks. Furthermore, scapolitization caused striking increase of HFS and LIL elements relative to free scapolite gabbros.

REFERENCES CITED

Ahmadi-Khalaji, A., Esmaeily, D., Valizadeh, M. V., et al., 2007. Petrology and Geochemistry of the Granitoid Complex of Boroujerd, Sanandaj-Sirjan Zone, Western Iran. *Journal of Asian Earth Sciences*, 29(56): 859–877

Alavi, M., 1994. Tectonics of the Zagros Orogenic Belt of Iran: New Data and Interpretations. *Tectonophysics*, 229(3–4): 211–238

Alavi, M., 2004. Regional Stratigraphy of the Zagros Fold-Thrust Belt of Iran and Its Proforeland Evolution. *American Journal of Science*, 304(1): 1–20

Baker, J., Newton, R. C., 1995. Experimentally Determined Activity-Composition Relations for Ca-Rich Scapolite in the System $CaAl_2Si_2O_8$-$NaAlSi_3O_8$-$CaCO_3$ at 7 kbar. *American Mineralogist*, 80: 744–751

Chamberlain, C. P., Docka, J. A., Post, J. E., et al., 1985. Scapolite: Alkali Atom Configurations, Antiphase Domains, and Compositional Variations. *American Mineralogist*, 70: 134–140

Eftekharnejad, J., 1973. 1 : 250 000 Geological Map of Mahabad. Geological Survey of Iran Press, Tehran

Ghalamghash, J., Nedelec, A., Bellon, H., et al., 2009. The Urumieh Plutonic Complex (NW Iran): A Record of the Geodynamic Evolution of the Sanandaj-Sirjan Zone during Cretaceous Times—Part I: Petrogenesis and K/Ar Dating. *Journal of Asian Earth Sciences*, 35(5): 401–415

Heltz, R. T., 1973. Phase Relations of Basalts in Their Melting Range at P_{H2O}=5 kb as a Function of Oxygen Fugacity-Part I. Mafic Phases. *Journal of Petrology*, 14(2): 249–302

Jiang, S. Y., Palmer, M. R., Xue, C. J., et al., 1994. Halogen-Rich Scapolite-Biotite Rocks from the Tongmugou Pb-Zn Deposit, Qinling, North-Western China: Implications for the Ore-Forming Process. *Mineralogical Magazine*, 58: 543–552

Komada, N., Moecher, D. P., Westrum, E. F., et al., 1996. Thermodynamic Properties of Scapolites at Temperatures Ranging from 10 K to 1 000 K. *Journal of Chemical Thermodynamics*, 28(9): 941–973

Kullerud, K., Erambert, M., 1999. Cl-Scapolite, Cl-Amphibole, and Plagioclase Equilibria in Ductile Shear Zones at Nusfjord, Lofoten, Norway: Implications for Fluid Compositional Evolution during Fluid-Mineral Interaction in the Deep Crust. *Geochimica et Cosmochimica Acta*, 63(22): 3829–3844

Leake, B. E., Woolley, A. R., Arps, C. E. S., et al., 1997. Nomenclature of Amphiboles: Report of the Subcommittee on Amphiboles of the International Mineralogical Association, Commission on New Minerals and Mineral Names. *Canadian Mineralogist*, 35: 219–246

Mazhari, S. A., 2008. Petrogenesis of Naqadeh-Sardasht Plutons: [Dissertation]. Tarbiat Moallem University, Tehran. 216

Mazhari, S. A., Bea, F., Amini, S., et al., 2009. The Eocene Bimodal Piranshahr Massif of the Sanandaj-Sirjan Zone, NW Iran: A Marker of the End of the Collision in the Zagros Orogen. *Journal of the Geological Society*, 166: 53–69

Morimoto, N., 1989. Nomenclature of Pyroxenes. *Canadian Mineralogist*, 27: 143–156

Otten, M. T., 1984. The Origin of Brown Hornblende in the Artfjaellet Gabbro and Dolerites. *Contributions to Mineralogy and Petrology*, 86(2): 189–199

Perchuck, L. L., Aranovich, L. Y., Podlesskii, K. K., et al., 1985. Precambrian Granulites of the Aldan Shield, Eastern Siberia, USSR. *Journal of Metamorphic Geology*, 3(3): 265–310

Seto, Y., Schimobayashi, N., Miyake, A., et al., 2004. Composition and $I4/m$-$P4_2/n$ Phase Transition in Scapolite Solid Solutions. *American Mineralogist*, 89: 257–265

Sun, S. S., McDonough, W. F., 1989. Chemical and Isotopic Systematics of the Oceanic Basalts: Implications for Mantle Composition and Processes: In: Saunder, A. D., Norry, M. J., eds., Magmatism in the Oceanic Basalts. *Geological Society*, 42: 313–345

Teertstra, D. K., Sherriff, B. L., 1997. Substitutional Mechanisms, Compositional Trends and the End-Member Formulae of Scapolite. *Chemical Geology*, 136(3–4): 233–260

Vanko, D. A., Bishop, F. C., 1982. Occurrence and Origin of Marialitic Scapolite in the Humboldt Lopolith, N.W. Nevada. *Contributions to Mineralogy and Petrology*, 81(4): 277–289